Inorg. Chem. **2008**, *47*, 4796−4807

DFT Calculation of $^{1}J(^{119}Sn,^{13}C)$ and $^{2}J(^{119}Sn,^{1}H)$ Coupling Constants in Di- and Trimethyltin(IV) Compounds

Girolamo Casella,[†] Francesco Ferrante,[‡] and Giacomo Saielli*[,§]

Dipartimento di Chimica Inorganica e Analitica "Stanislao Cannizzaro", Università di Palermo, Viale delle Scienze, Parco D'Orleans II, Ed. 17, 90128 Palermo, Italy, Dipartimento di Chimica Fisica "Filippo Accascina", Università di Palermo, Viale delle Scienze, Parco D'Orleans II, Ed. 17, 90128 Palermo, Italy, and Istituto per la Tecnologia delle Membrane del CNR, Sezione di Padova, Via Marzolo 1, 35131 Padova, Italy

Received January 18, 2008

We have tested several computational protocols, at the nonrelativistic DFT level of theory, for the calculation of $^{1}J(^{119}Sn,^{13}C)$ and $^{2}J(^{119}Sn,^{1}H)$ spin−spin coupling constants in di- and trimethyltin(IV) derivatives with various ligands. Quite a good agreement with experimental data has been found with several hybrid functionals and a double-ζ basis set for a set of molecules comprising tetra-, penta-, and hexa-coordinated tin(IV). Then, some of the protocols have been applied to the calculation of the $^{2}J(^{119}Sn,^{1}H)$ of the aquodimethyltin(IV) ion and dimethyltin(IV) complex with D-ribonic acid and to the calculation of $^{1}J(^{119}Sn,^{13}C)$ and $^{2}J(^{119}Sn,^{1}H)$ of the dimethyltin(IV)−glycylglycine and glycylhistidine complexes in water solutions. Solvent effects have been considered in these cases by including explicit water molecules and/or the solvent reaction field, resulting in a good agreement with experimental data. The proposed protocols constitute a helpful tool for the structural determination of di- and triorganotin(IV) derivatives.

Introduction

Most of the extensive use of organotin(IV) derivatives arises from their activity toward several biological targets.[1,2] Their application as potential antitumor agents is, in fact, also actively investigated,[3–5] and several recent experimental studies, concerning the interaction of alkyltin(IV) compounds with model systems like nucleotides,[6] aminoacids[7] and peptides,[8] are aimed at elucidating the detailed molecular mechanism of their biological activity.

Among many techniques used to study the structure and reactivity of organotin(IV) compounds in solution phase, ^{119}Sn NMR plays a central role due to the favorable magnetic properties of the ^{119}Sn nucleus, that is $I = {}^{1}/_{2}$ and a relative receptivity, with respect to ^{13}C, of 25.2.[9,10] ^{1}H and ^{13}C NMR are the other essential tools for the characterization of organotin(IV) derivatives. NMR methodologies, as applied to the advanced structure determination of tin compounds, have been thoroughly described.[11]

Together with the tin chemical shift,[12–15] spin−spin coupling constants $^{n}J(^{119}Sn, X)$ ($n = 1, 2, 3$; X = ^{1}H, ^{2}H,

* To whom correspondence should be addressed. E-mail: giacomo.saielli@unipd.it.
† Dipartimento di Chimica Inorganica e Analitica, Università di Palermo.
‡ Dipartimento di Chimica Fisica, Università di Palermo.
§ ITM-CNR, Sezione di Padova.

(1) Smith, P. J. *Chemistry of Tin*; Chapman & Hall: London, 1998.
(2) Pellerito, L.; Nagy, L. *Coord. Chem. Rev.* **2002**, *224*, 111–150.
(3) Saxena, A. K.; Huber, F. *Coord. Chem. Rev.* **1989**, *95*, 109–123.
(4) (a) Gielen, M. *Coord. Chem. Rev.* **1996**, *151*, 41–51. (b) Gielen, M. *Appl. Organomet. Chem.* **2002**, *16*, 481–494. (c) Gielen, M.; Biesemans, M.; Willem, R. *Appl. Organomet. Chem.* **2005**, *19*, 440–450.
(5) Yang, P.; Guo, M. *Coord. Chem. Rev.* **1999**, *185*−*186*, 189–211.
(6) (a) Ghys, L.; Biesemans, M.; Gielen, M.; Garoufis, A.; Hadjiliadis, N.; Willem, R.; Martins, J. C. *Eur. J. Inorg. Chem.* **2000**, 513–522. (b) Cassus, E. P.; Machado, S. P.; Wardell, J. L *Appl. Organomet. Chem.* **2007**, *21*, 203–208.
(7) (a) Surdy, P.; Rubini, P.; Buzás, N.; Henry, B.; Pellerito, L.; Gajda, T *Inorg. Chem.* **1999**, *38*, 346–352. (b) Ma, C.; Zhang, J.; Zhang, R. *Heteroatom Chem.* **2003**, *14*, 637–641.
(8) (a) Buck, B.; Mascioni, A.; Que, L.; Veglia, L *J. Am. Chem. Soc.* **2003**, *125*, 13316–13317. (b) Buck, B.; Mascioni, A.; Cramer, C. J.; Veglia, L. *J. Am. Chem. Soc.* **2004**, *126*, 14400–14410.
(9) (a) Mason, J. *Multinuclear NMR*; Plenum Press: New York, 1987. (b) Gielen, M.; Willem, R.; Wrackmeyer, B. *Advanced Applications of NMR to Organometallic Chemistry*; John Wiley and Sons, Ltd.: Chichester, U.K., 1996.
(10) Davies, A. G. *Organotin Chemistry*; VCH: Weinheim, Germany, 1997.
(11) Martins, J. C.; Biesemans, M.; Willem, R. *Prog. NMR Spectrosc.* **2000**, *36*, 271–322.
(12) Smith, P. J.; Tupčiauskas, A. P. *Annu. Rep. NMR Spectrosc.* **1978**, *8*, 291–370.
(13) Hani, R.; Geanagel, R. A. *Coord. Chem. Rev.* **1982**, *44*, 229–246.
(14) Wrackmeyer, B. *Annu. Rep. NMR Spectrosc.* **1985**, *16*, 73–186.
(15) Wrackmeyer, B. *Annu. Rep. NMR Spectrosc.* **1999**, *38*, 203–264.

10.1021/ic8000976 CCC: $40.75
Published on Web 05/06/2008

^{13}C) have proven to be a powerful tool in the determination of the structure of organotin(IV) derivatives.[9b,16–23] In particular, for di- and trimethyltin(IV) compounds, empirical relationships between $^1J(^{119}Sn,^{13}C)$ or $^2J(^{119}Sn,^1H)$ and the corresponding C−Sn−C angle, θ, have been proposed by Lockhart et al.[16–18] Comparison between structural X-ray data with ^1Js obtained by solid-state NMR measurements, led to eq 1;[16] the estimation of θ in solution, by eq 1, and the comparison with the corresponding ^2Js, provided a second relationship, eq 2;[17] finally, by using an extended set of data, a slightly improved version of eq 1 was proposed, eq 3.[18]

$$|^1J| = 11.4\theta - 875 \quad (1)$$

$$\theta = 0.0161|^2J|^2 - 1.32|^2J| + 133.4 \quad (2)$$

$$|^1J| = (10.7 \pm 0.5)\theta - (778 \pm 64) \quad (3)$$

Eqs 1–3 allow us to correlate the coordination pattern of tin(IV) in di- and trimethyltin(IV) derivatives with the $^{1,2}J$ coupling constants: in tetra-coordinated tin compounds ($\theta \leq 112°$) ^1Js are predicted to be smaller than about 400 Hz, whereas ^2Js should be below 60 Hz; for penta-coordinated tin ($\theta = 115-130°$), ^1Js fall in the 450−670 Hz range and the ^2Js fall in the 65−80 Hz range; finally, for hexa-coordinated tin ($\theta \geq 135°$) ^1Js and ^2Js are generally larger than 670 and 83 Hz, respectively.[17] We note that these ranges are just a qualitative indication and overlaps among the tin coordination intervals may occur.[17] However, marked deviations from the values predicted by eqs 1–3 are not unusual:[17] for hexa-coordinated *cis*-dimethyltin(IV) derivatives, the value of θ predicted from eq 1 or eq 3 (using ^1J) and eq 2 (using ^2J) is often larger than the experimental value, and dimethyltin(IV) halides follow a slightly different equation.[17]Also, in trimethyltin(IV) compounds, some ^1Js appeared to be not so well correlated with the local coordination at tin.[18]

Whereas these exceptions may suggest unusual configurations of methyltin(IV) derivatives, they reveal, as also stressed in refs[17] and,[18] the empirical nature of eqs 1–3. Nevertheless, they are still widely used in the NMR structural determination of di- and trimethyltin(IV) compounds, refs[6–8] and ref. [24] for recent examples; it is therefore useful to look for a general quantum chemical protocol to validate the aforementioned relationships, and, most importantly, one which should be able to predict the $^{1,2}J$s coupling constants of putative structures to be compared with experimental data.

In recent years, increasing effort has been devoted to the calculation of ^{119}Sn NMR parameters by quantum chemical methods, and, in this respect, DFT has emerged as a useful methodology to support and/or predict experimental data. Concerning the ^{119}Sn shielding tensor, nonrelativistic DFT approaches give values that generally correlate well with the experimental data[25–28] also when the comparison is done with experiments conducted in coordinating solvents like water.[29,30] When several heavy halogen atoms are bound to tin, the spin−orbit (SO) coupling contribution becomes not negligible and its inclusion in the Hamiltonian is mandatory.[28,31] The calculation of coupling constants has been found to be subject to large scalar relativistic effects already for moderately heavy nuclei and even more so for heavier nuclei.[32,33] For tin, relativistic calculations at the DFT level of $^nJ(^{119}Sn,X)$ (n = 1, 2, 3; X = ^{1}H, ^{13}C) have been reported.[28,34,35] However, fully satisfactory results have not been obtained so far. For example, relativistic DFT calculations at the scalar and spin−orbit level, within the ZORA formalism, underestimated $^1J(^{119}Sn,^{13}C)$ and $^2J(^{119}Sn,^1H)$ by a factor of about 3.[28]

In this work, we approach the problem from a more practical point of view: we present a nonrelativistic GIAO-DFT computational study of $^1J(^{119}Sn,^{13}C)$ and $^2J(^{119}Sn,^1H)$ in di- and trimethyltin(IV) derivatives where several functionals have been tested. Although relativistic effects have been neglected, some of the investigated protocols have a high predictive power. Moreover, we report some applications of the computational protocols to the aquodimethyltin(IV) ion and to some compounds of biological interest, namely complexes of dimethyltin(IV) with D-ribonic acid and with glycylglycine and glycylhistidine dipeptides. In these cases, because experimental data have been collected in water, solvent effects are expected to play a significant role on the NMR properties.[36] Therefore, explicit water molecules and/or long-range solvent effects have been considered in the computational protocols.

(16) Lockhart, T. P.; Manders, W. F.; Zuckerman, J. J. *J. Am. Chem. Soc.* **1985**, *107*, 4546–4547.
(17) Lockhart, T. P.; Manders, W. F. *Inorg. Chem.* **1986**, *25*, 892–895.
(18) Lockhart, T. P.; Manders, W. F. *J. Am. Chem. Soc.* **1987**, *109*, 7015–7020.
(19) Holeček, J.; Lyčka, A. *Inorg. Chim. Acta* **1986**, *118*, L15–L16.
(20) Holeček, J.; Nadvornik, M.; Handlir, K.; Lyèka, A. *J. Organomet. Chem.* **1986**, *315*, 299–308.
(21) Quintard, J. P.; Degueil-Castaing, M.; Dumartin, G.; Barbe, B.; Petraud, M. *J. Organomet. Chem.* **1982**, *234*, 27–40.
(22) Quintard, J. P.; Degueil-Castaing, M.; Barbe, B.; Petraud, M. *J. Organomet. Chem.* **1982**, *234*, 41–61.
(23) Mitchell, T. N.; Podesta, J. C.; Ayala, A.; Chopa, A. B. *Magn. Reson. Chem.* **1988**, *26*, 497–500.
(24) (a) Casas, J. S.; Castineiras, A.; Condori, F.; Couce, M. D.; Russo, U.; Sánchez, A.; Sordo, J.; Varela, J. M.; Vazquez Lopez, E. M. *J. Organomet. Chem.* **2007**, *692*, 3547–3554. (b) Casas, J. S.; Castellano, E. E.; Couce, M. D.; Ellena, J.; Sánchez, A.; Sánchez, J. L.; Sordo, J.; Taboada, C. *Inorg. Chem.* **2004**, *43*, 1957–1963.
(25) Vivas-Reyes, R.; De Proft, F.; Biesemans, M.; Willem, R.; Geerlings, P. *J. Phys. Chem. A* **2002**, *106*, 2753–2759.
(26) Avalle, P.; Harris, R. K.; Fischer, R. D. *Phys. Chem. Chem. Phys.* **2002**, *4*, 3558–3561.
(27) Avalle, P.; Harris, R. K.; Kardakov, P. B.; Wilson, P. J. *Phys. Chem. Chem. Phys.* **2002**, *4*, 5925–5932.
(28) Bagno, A.; Casella, G.; Saielli, G. *J. Chem. Theory Comput.* **2006**, *2*, 37–46.
(29) Bagno, A.; Bertazzi, N.; Casella, G.; Pellerito, L.; Saielli, G.; Sciacca, I. D. *J. Phys. Org. Chem.* **2006**, *19*, 874–883.
(30) Bertazzi, N.; Casella, G.; Ferrante, F.; Pellerito, L.; Rotondo, A.; Rotondo, E. *Dalton Trans.* **2007**, *14*, 1440–1446.
(31) Kaneko, H.; Hada, M.; Nakajima, T.; Nakatsuji, H. *Chem. Phys. Lett.* **1996**, *261*, 1–6.
(32) Kaupp, M.; Bühl, M.; Malkin, V. G. *Calculation of NMR and EPR Parameters*; Wiley-VCH: Weinheim, Germany, 2004.
(33) Bryce, D. L.; Wasylishen, R. E.; Autschbach, J.; Ziegler, T. *J. Am. Chem. Soc.* **2002**, *124*, 4894–4900.
(34) Khandogin, J.; Ziegler, T. *J. Phys. Chem. A* **2000**, *104*, 113–120.
(35) Oprea, C. I.; Rinkevicius, Z.; Vahtras, O.; Ågren, H.; Ruud, K. *J. Chem. Phys.* **2005**, *123*, 014101−014111.
(36) Bagno, A.; Rastrelli, F.; Saielli, G. *Prog. NMR Spectrosc.* **2005**, *47*, 41–93.

Computational Methods

Calculations were performed at the nonrelativistic DFT level; geometry optimizations were run using the popular three-parameters hybrid functional B3LYP[37] and also with the PBE1PBE[38] functional because the latter gave the best agreement with the experimental Sn−C distance of tetramethylstannane (TMSn) (Results and Discussion section). The 6-31G(d,p) basis set was used for all of the atoms except for tin, for which the all-electron DZVP[39] basis set (contraction scheme: (18s14p9d)/[6s5p3d]) was employed. For the calculation of the spin−spin coupling constants, several functionals (Results and Discussion section), in conjunction with the gauge independent atomic orbital (GIAO) formalism, were used with the same basis sets as for the optimizations. For the set of molecules optimized with the B3LYP functional, containing phosphorus, sulfur, chlorine, and selenium atoms, additional calculations were performed using the 6-311G(d,p) basis set for these atoms. An integration grid of 99 radial shells and 302 angular points were used both for the optimizations and for the spin−spin coupling constants calculation. In some cases, long-range solvent effects have been included using the PCM[40] formalism. For TMSn, we have checked the effect of uncontracting the basis set and adding tight polarization functions for the core, thus using a spherical product integration grid of 4×10^6 points per atom (200 radial shells, with 100 θ points and 200 ϕ points each). All contributions to the couplings have been evaluated, namely the spin-dipole, diamagnetic, and paramagnetic spin−orbit and Fermi-contact terms. They are reported in the Supporting Information, whereas only the total spin−spin coupling constant is discussed in the main text. All calculations were run using the *Gaussian 03* package.[41] Except for the glycylhistidine complex, where the two methyl groups are nonequivalent, all calculated *J*s are averaged over the two, or three, methyl groups. In the application to systems of biological interest, $^2J(^{119}\mathrm{Sn},^1\mathrm{H})$ couplings always refer to the methyl groups; other protons, namely protons of coordinated water molecules or NH_2 groups, are exchanged with the solvent and not coupled to tin.

Table 1. Calculated Sn−C Bond Distance, *d* (pm)

functional	*d*(Sn−C)	Δd^a
BP86[43,44]	219.0	4.6
BLYP[43,45]	220.8	6.4
PBEPBE[46]	218.5	4.1
PW91PW91[47]	218.3	3.9
OLYP[45,48]	218.9	4.5
OPW91[47,48]	217.2	2.8
G96LYP[45,49]	220.6	6.2
B3PW91[50]	217.4	3.0
B3LYP[37]	218.5	4.1
PBE1PBE[38]	216.4	2.0
B971[51]	218.1	3.7
B98[52]	218.2	3.8
mPWB1K[53]	220.7	6.3
mPW1PW91[54]	216.8	2.4
B3P86[51]	216.8	2.4
O3LYP[55]	218.7	4.3
mPW3LYP[56]	218.4	4.0

[a] $d_{calc} - d_{exp}$, experimental distance is 214.4 pm.[42]

Results and Discussion

Tetramethylstannane Test Case. A preliminary investigation has been carried out to test the performance of a set of pure and hybrid functionals for the geometry optimization of tetramethylstannane, TMSn. Results are reported in Table 1. All the functionals we have considered overestimate the Sn−C bond distance, some by more than 6 pm, compared to the experimental value;[42] a somewhat better performance is found for the PBE1PBE functional, which is off by only 2 pm. Therefore, a first set of geometry optimizations has been run with the widely used B3LYP functional and a second set with the PBE1PBE functional.

Next, calculations of $^1J(^{119}\mathrm{Sn},^{13}\mathrm{C})$ and $^2J(^{119}\mathrm{Sn},^1\mathrm{H})$ of TMSn have been performed using (i) the experimental

(37) (a) Stephens, P. J.; Devlin, F. J.; Chabalowski, C. F.; Frisch, M. J. *J. Phys. Chem.* **1994**, *98*, 11623–11627. (b) Hertwig, R. H.; Koch, W. *Chem. Phys. Lett.* **1997**, *268*, 345–351.

(38) (a) Perdew, J. P.; Burke, K.; Ernzerhof, M. *Phys. Rev. Lett.* **1996**, *77*, 3865–3868. (b) Perdew, J. P.; Burke, K.; Ernzerhof, M. *Phys. Rev. Lett.* **1997**, *78*, 1396–1396.

(39) (a) Godbout, N.; Salahub, D. R.; Andzelm, J.; Wimmer, E. *Can. J. Chem.* **1992**, *70*, 560–571. (b) Schuchardt, K. L.; Didier, B. T.; Elsethagen, T.; Sun, L.; Gurumoorthi, V.; Chase, J.; Li, J.; Windus, T. L. *J. Chem. Inf. Model.* **2007**, 1045–1052.

(40) (a) Cancès, M. T.; Mennucci, B.; Tomasi, J. *J. Chem. Phys.* **1997**, *107*, 3032–3041. (b) Cossi, M.; Barone, V.; Mennucci, B.; Tomasi, J. *Chem. Phys. Lett.* **1998**, *286*, 253–260. (c) Mennucci, B.; Tomasi, J. *J. Chem. Phys.* **1997**, *106*, 5151–5158.

(41) Frisch, M. J. ; Trucks, G. W.; Schlegel, H. B.; Scuseria, G. E.; Robb, M. A.; Cheeseman, J. R.; Montgomery Jr., J. A.; Vreven, T.; Kudin, K. N.; Burant,J. C.; Millam, J. M.; Iyengar, S. S.; Tomasi, J.; Barone, V.; Mennucci, B.; Cossi, M.; Scalmani, G.; Rega, N.; Petersson, G. A.; Nakatsuji, H.; Hada, M.; Ehara, M.; Toyota, K.; Fukuda, R.; Hasegawa, J.; Ishida, M.; Nakajima, T.; Honda, Y.; Kitao,O.; Nakai, H.; Klene, M.; Li, X.; Knox, J. E.; Hratchian, H. P.; Cross, J. B.; Bakken, V.; Adamo, C.; Jaramillo, J.; Gomperts, R. ; Stratmann,R. E. ; Yazyev,O. ; Austin,A. J. ; Cammi, R. ; Pomelli,C. ; Ochterski, J. W.; Ayala,P. Y.; Morokuma, K.; Voth, G. A.; Salvador, P.; Dannenberg, J. J.; Zakrzewski, V. G.; Dapprich, S.; Daniels, A. D.; Strain, M. C.; Farkas, O.; Malick, D. K.; Rabuck, A. D.; Raghavachari, K.; Foresman, J. B.; Ortiz, J. V.; Cui, Q.; Baboul,A. G.; Clifford, S.; Cioslowski, J.; Stefanov, B. B.; Liu, G.; Liashenko, A.; Piskorz, P.; Komaromi, I.; Martin, R. L.; Fox, D. J.; Keith, T.; Al-Laham, M. A.; Peng, C. Y.; Nanayakkara,A.; Challacombe, M.; Gill, P. M. W.; Johnson, B.; Chen, W.; Wong, M. W.; Gonzalez, C.; Pople, J. A., *Gaussian 03*, Revision D.02; Gaussian, Inc.: Wallingford, CT, 2004.

(42) (a) Cremer, D.; Olsson, L.; Reichel, F.; Kraka, E. *Isr. J. Chem.* **1993**, *33*, 369–385. (b) Vilkov, L. V.; Mastryukov, V. S.; Sadova, N. I. *Determination of the Geometrical Structure of Free Molecules*; Mir Publisher: Moscow, 1983. (c) Wilkinson, G. R.; Wilson, M. K. *J. Chem. Phys.* **1956**, *25*, 784–784. (d) Beagley, B.; McAloon, K.; Freeman, J. M. *Acta Crystallogr. B* **1974**, *30*, 444–449. (e) Clark, H. C.; Furnival, S. G.; Kwon, J. T. *Can. J. Chem.* **1963**, *41*, 2889–2897. (f) Fujii, H.; Kimura, M. *Bull. Chem. Soc. Jpn.* **1970**, *44*, 2643–2647.

(43) Becke, A. D. *Phys. Rev. A* **1998**, *38*, 3098–3100.

(44) Perdew, P. J. *Phys. Rev. B* **1986**, *33*, 8822–8824.

(45) (a) Lee, C.; Yang, W.; Parr, G. *Phys. Rev. B* **1988**, *37*, 785–789. (b) Miehlich, B.; Savin, A.; Stoll, H.; Preuss, H. *Chem. Phys. Lett.* **1989**, *157*, 200–206.

(46) Perdew, J. P.; Burke, K.; Ernzerhof, M. *Phys. Rev. Lett.* **1996**, *77*, 3865–3868.

(47) (a) Perdew, J. P.; Chevary, J. A.; Vosko, S. H.; Jackson, K. A.; Pederson, M. R.; Fiolhais, C. *Phys. Rev. B* **1992**, *46*, 6671–6687. (b) Perdew, J. P.; Chevary, J. A.; Vosko, S. H.; Jackson, K. A.; Pederson, M. R.; Fiolhais, C. *Phys. Rev. B* **1993**, *48*, 4978. (c) Perdew, J. P.; Burke, K.; Wang, Y. *Phys. Rev. B* **1996**, *54*, 16533–16539.

(48) Handy, N. C.; Cohen, A. J. *Mol. Phys.* **2001**, *99*, 403–412.

(49) (a) Gill, P. M. W. *Mol. Phys.* **1996**, *89*, 433–445. (b) Adamo, C.; Barone, V. *J. Com. Chem.* **1998**, *19*, 418–429.

(50) Becke, A. D. *J. Chem. Phys.* **1993**, *98*, 5648–5652.

(51) (a) Becke, A. D. *J. Chem. Phys.* **1997**, *107*, 8554–8560. (b) Hamprecht, F. A.; Cohen, A. J.; Tozer, D. J.; Handy, N. C. *J. Chem. Phys.* **1998**, *109*, 6264–6271.

(52) Schmider, H. L.; Becke, A. D. *J. Chem. Phys.* **1998**, *108*, 9624–9631.

(53) (a) Adamo, C.; Barone, V. *J. Chem. Phys.* **1998**, *108*, 664–675. (b) Lynch, B. J.; Zhao, Y.; Trulhar, D. G. J. *Phys. Chem. A* **2003**, *107*, 1384–1388.

(54) Zhao, Y.; Truhlar, D. G. *J. Phys. Chem. A* **2004**, *108*, 6908–6918.

(55) Hoe, W.; Cohen, A. J.; Handy, N. C. *Chem. Phys. Lett.* **2001**, *341*, 319–328.

(56) Zhao, Y.; Truhlar, D. G. *J. Phys. Chem. A* **2004**, *108*, 6908–6918.

Table 2. Calculated $^1J(^{119}Sn,^{13}C)$ and $^2J(^{119}Sn,^1H)$ Coupling Constants (Hz) of TMSn with Different Functionals

pure functionals	^1J ($^{119}Sn,^{13}C$)[a]	^2J ($^{119}Sn,^1H$)[a]	hybrid functionals	^1J ($^{119}Sn,^{13}C$)[a]	^2J ($^{119}Sn,^1H$)[a]
BP86	−279.1	34.9	B3PW91	−353.4	48.1
BLYP	−289.0	28.2	B3LYP	−351.3	39.7
PBEPBE	−288.5	34.0	PBE1PBE	−372.7	50.6
PW91PW91	−286.4	34.9	B971	−352.4	36.5
OLYP	−322.0	43.1	B98	−359.5	40.9
OPW91	−322.4	52.6	mPW1PW91	−373.5	52.9
G96LYP	−284.6	32.7	mPWB1K	−393.1	49.6
			B3P86	−345.9	45.6
			O3LYP	−354.0	47.3
			mPW3LYP	−350.5	38.8
exptl [b]	−336.9	54.7	exptl [b]	−336.9	54.7

[a] Fully optimized geometry at the B3LYP level. [b] From ref.[57]

geometry, which is a geometry where the Sn−C distance was kept frozen at the experimental value of 214.4 pm[42] while hydrogen positions were optimized, and (ii) a fully optimized geometry. B3LYP and PBE1PBE functionals have been used in both cases for optimization.

In Table 2, we report the results obtained for the fully optimized geometry (B3LYP). Full data can be found in the Supporting Information (Tables S1 and S2 and Figures S1−S4). There is a significant dependence on the functional used for the spin−spin coupling calculation: for example, the calculated ^1Js using BP86 or mPWB1K differ by more than 100 Hz, and the calculated ^2Js using BLYP and mPW1PW91 differ by almost 25 Hz. Moreover, it seems rather difficult to single out a functional performing better than the others for both ^1Js and ^2Js, although OPW91 seems rather good for both couplings and hybrid functionals appear to perform generally better than pure functionals for ^2J. We also note that pure functionals generally underestimate (in magnitude) ^1J, whereas hybrid functionals overestimate it.

The coupling constants calculated using the uncontracted basis set augmented with tight polarized core functions are smaller, in magnitude, than those obtained with the standard basis set. This is particularly evident for ^1J. For example, using the BLYP functional and the experimental Sn−C distance we obtain $^1J(^{119}Sn,^{13}C) = -195.6$ Hz and $^2J(^{119}Sn,^1H) = 26.5$ Hz. These values should be compared with the analogous scalar ZORA relativistic results, obtained using large Slater-type basis sets, of −164.6 and 10.0 Hz, respectively[28] (see also Table S1 in the Supporting Information). Thus, by increasing the flexibility of the basis set the results seem to converge to the values obtained at the relativistic level.

As mentioned in the Introduction and discussed in ref,[28] high level calculation significantly underestimates the coupling constants compared to the experimental values, a puzzling result worthy of a deeper theoretical investigation. Thus, for the purpose of defining a practical computational tool to be used as an aid in structural assignment, also considering the high computational cost of using the large basis set, we select the standard basis set for the following calculations on large organotin(IV) complexes.

(57) (a) Kerschl, S.; Sebald, A.; Wrackmeyer, B. *Magn. Reson. Chem.* **1985**, *23*, 514–520. (b) Petrosyan, V. S.; Permin, A. B.; Reutov, O. A. *J. Magn. Reson.* **1980**, *40*, 511–518.

Finally, on the basis of their performance (Table 2 and in the Supporting Information, Tables S1 and S2 and Figures S1−S4) we have selected some functionals to test their predictive power using a more extended set of molecules taken from ref[17] and shown in Scheme 1. These are: OPW91, B3PW91, B3LYP, PBE1PBE, mPW1PW91, B3P86, and O3LYP. The set of selected molecules allowed to calculate $^{1,2}J$s for the most common coordination environments observed in organotin(IV) compounds, namely tetra-, penta-, and hexa-coordination, thus covering a broad range of values for ^1J and ^2J of 800 and 50 Hz, respectively. Experimental data have been selected from results obtained in noncoordinating solvents.

Model Systems with B3LYP Geometries. In the Supporting Information (Tables S3 and S4), we report the calculated $^1J(^{119}Sn,^{13}C)$ and $^2J(^{119}Sn,^1H)$ for the set of molecules and selected functionals mentioned above. The correlation between experimental and calculated data is shown in Figures 1 and 2, respectively. The negative slope in Figure 1 is due to the fact that the calculated, negative, ^1J coupling constant is correlated with the absolute value of the experimental one. In fact, whereas the sign of ^1J for the investigated structures should be always negative,[9b] there is a lack of data for most of them. We note that calculated ^1Js using the OPW91 functional are in good agreement with experimental values for tetra-coordinated tin(IV) derivatives, as noted already. However. this appears to be fortuitous because significant deviations are found for the larger coupling constants of penta- and hexa-coordinated tin compounds. The remaining functionals, instead, seem to be rather good, all having a correlation slope close to −1 (see Table 3 with statistical correlation parameter) and therefore a high predictive power. In particular, B3LYP appears to be one of the best functionals for the calculations of ^1Js (best fit and one of the lowest mean absolute errors, MAE, and maximum absolute errors, E_{max}), but it is quite in error concerning the ^2Js (poor fit and high MAE and E_{max}). It is, therefore, not possible to single out just one functional giving accurate results for both ^1Js and ^2Js. However, on the basis of the statistical parameters and the maximum absolute errors reported in Table 3, it seems that the mPW1PW91 functional is the best compromise to obtain accurate values of both coupling constants.

We also note (Supporting Information) that the DSO contribution to ^1J is negligible: in all cases investigated it is on the order of 0.25 Hz; the PSO term is, instead, significant on the order of 15 Hz, and it does not seem to be strongly influenced by the coordination pattern of tin; the SD contribution is always negative, about −10 Hz, therefore partly canceling the PSO term; the FC term is, by far, the largest contribution and it is also significantly affected by tin coordination. A similar trend is observed for ^2J: the DSO contribution is negligible (less than 0.25 Hz), the PSO term is on the order of 2.5 Hz, the SD term is on the order of −1 Hz; these contributions are not strongly dependent on tin coordination. Also for ^2J, the dominant contribution, depending on tin coordination, is the Fermi-contact term.

Scheme 1. Model Systems Investigated

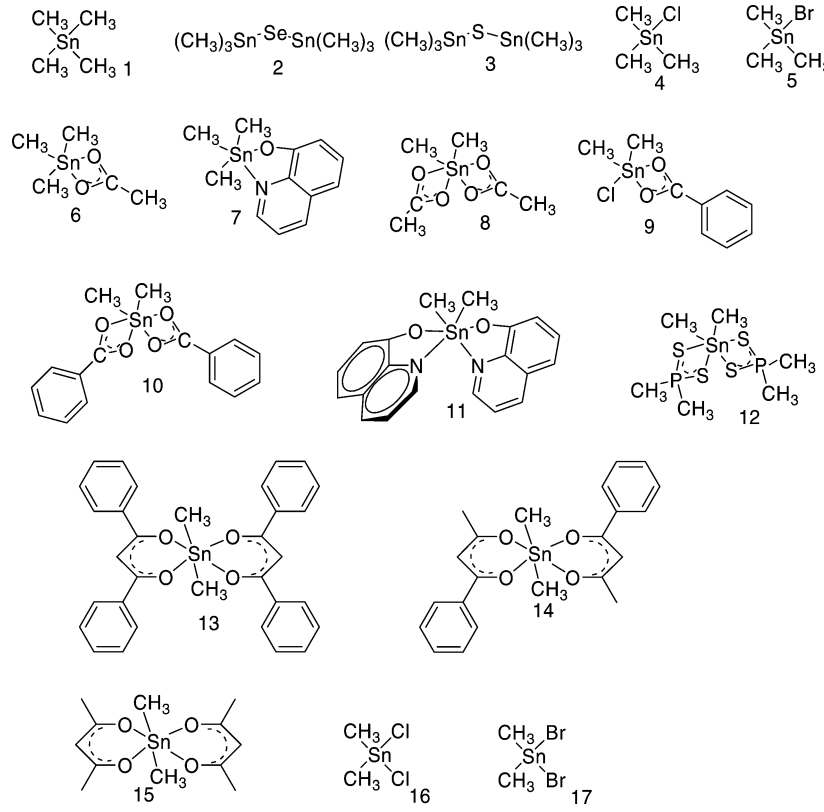

***cis*-$Me_2Sn(IV)Ch_2$ species.** Hexa-coordinated *cis*-$Me_2Sn(IV)Ch_2$ (Ch = chelating ligand) complexes show interesting behavior concerning the dependence of $^{1,2}J$s on θ. The measured ^1Js and ^2Js for this class of compounds, in fact, are generally smaller than the values expected for a coordination number of six. On the other hand, they appear too large considering the small C−Sn−C angle, generally in the 109°−116° range, due to the double chelation experienced by the organotin(IV) moiety.[58] Thus, eqs 1–3 fail to correlate the $^{1,2}J$s with the experimental θ value as reported in ref[17] concerning **11** and the dimethyltin(IV)-*bis*-tropolonate complex ($Me_2Sn(Trop)_2$). Then, we deemed interesting to investigate these two compounds in more detail to check the goodness of the protocol also when this peculiar methyl configuration occurs. Moreover, we have also calculated the $^{1,2}J$s for the (dicyanoethylene-1,2-dithiolo)(1,10-phenanthroline)dimethyltin(IV) complex (($Me_2Sn(Phen)$-(mnt)); this, besides having a cis dimethyl configuration, offers the opportunity to investigate dithiolate complexes as models of the alkyltin(IV)−sulfur interaction in proteins.

The X-ray structure of $Me_2Sn(Ox)_2$ has been reported,[59] and further studies confirmed that the solid-state configuration is retained also in solution;[60] for $Me_2Sn(trop)_2$, very recent X-ray data are available[61] that confirm previous results;[62] finally, for ($Me_2Sn(Phen)$(mnt), X-ray data and solution-state ^2J have been recently reported.[63]

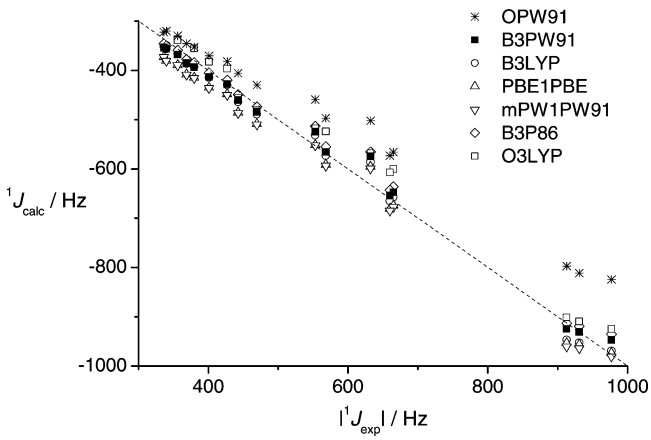

Figure 1. Correlation between calculated and experimental $^1J(^{119}Sn,^{13}C)$ of model systems of Scheme 1, B3LYP optimized geometries (Table S3 in the Supporting Information). (Dashed line) ideal correlation $y = -x$.

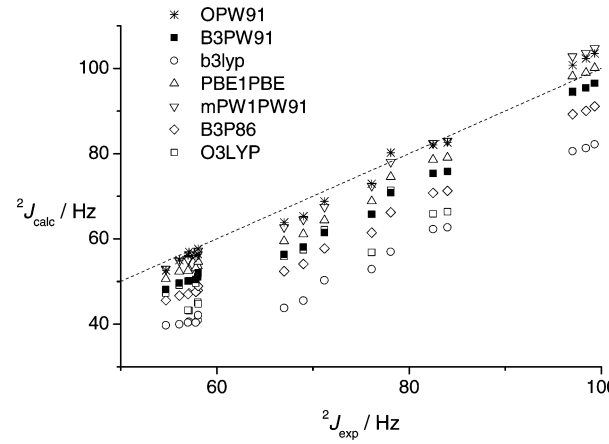

Figure 2. Correlation between calculated and experimental $^2J(^{119}Sn,^1H)$ of model systems of Scheme 1, B3LYP optimized geometries (Table S4 in the Supporting Information). (Dashed line) ideal correlation $y = x$.

Table 3. Statistical Correlation Parameters of $^1J(^{119}Sn,^{13}C)$ and $^2J(^{119}Sn,^1H)$ Data, B3LYP Geometries: Linear Fit $J_{calc} = a + bJ_{exp}$, Correlation Coefficient, R^2, Mean Absolute Error, MAE, Defined as $\Sigma_n|J_{calcd} - J_{exptl}|/n$, and Maximum Absolute Error, E_{max}

	$^1J(^{119}Sn,^{13}C)$					$^2J(^{119}Sn,^1H)$				
func.	*a* (Hz)	*b*	R^2	MAE (Hz)	E_{max} (Hz)	*a* (Hz)	*b*	R^2	MAE (Hz)	E_{max} (Hz)
OPW91	−41.2	−0.8058	0.9907	66.4	152.3	−8.33	1.1093	0.9894	2.12	4.15
B3PW91	−26.6	−0.9513	0.9916	16.2	57.7	−12.64	1.0778	0.9829	7.06	10.92
B3LYP	−12.3	−0.9900	0.9923	16.4	45.5	−16.12	0.9631	0.9663	18.77	23.51
PBE1PBE	−45.3	−0.9603	0.9913	28.3	42.3	−11.30	1.1013	0.9842	4.32	7.89
mPW1PW91	−42.0	−0.9719	0.9913	30.2	47.8	−11.55	1.1509	0.9859	2.63	5.82
B3P86	−20.0	−0.9453	0.9916	16.3	66.4	−12.22	1.0177	0.9789	10.95	14.91
O3LYP	−17.2	−0.9306	0.9851	30.1	54.7	−18.95	1.1187	0.9318	10.42	19.28

Scheme 2. Isomer Models of $Me_2Sn(Ox)_2$

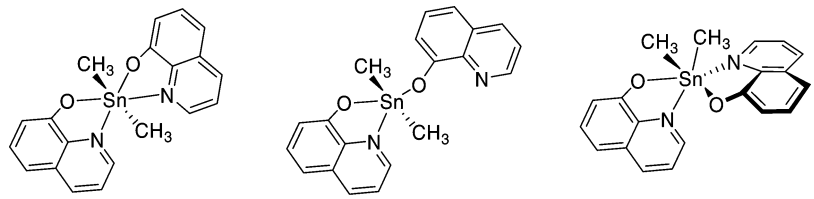

11a 11b 11c

For **11**, we considered different isomers (Scheme 2), namely: hexa-coordinated tin(IV) with the methyl groups arranged in trans configuration (**11a**); a penta-coordinated tin(IV) where the double chelation is lost (**11b**); a hexa-coordinated tin(IV) with cis methyl groups (**11c**, corresponding to the experimental geometry); the X-ray structure, except for the minimization of hydrogen positions (**11d**). Results for two other isomeric models of **11**, namely **11a′** and **11c′**, differing in the relative position of the donor atoms, oxygen and nitrogen, have been included in the Supporting Information.

Relevant structural data and calculated $^{1,2}J$s are reported in Table 4. We note that the largest calculated $^{1,2}J$ corresponds to the model with the largest value of θ (**11a**), consistent with the increased *s* character of the Sn−C bond. It is noteworthy that only the **11a** and **11b** models show the correlation $^{1,2}J$ versus θ as predicted by eqs 1–3, whereas the calculated results for **11c** differ from the expected values. However, calculated $^{1,2}J$s for **11a** are in disagreement with experimental values, whereas the calculated coupling constants for **11c** (the experimental isomer) are, instead, in good agreement. Model **11b** needs to be discussed in more detail. It may be formally considered as the turning point between *cis*-(**11a**) and *trans*-(**11c**) methyl configurations of **11**. In fact, in this case tin is penta-coordinated because one of the two ligands is no longer acting as a chelating agent. The lack of the structural constraint due to the double chelation allows the methyl groups to relax from the cis arrangement, restoring the $^{1,2}J$ dependence on θ as predicted by eqs 1–3. This explains the good agreement of the calculated $^{1,2}J$s (Table 4) with the experimental values and also points to the fact that for the hexa-coordinated *cis*-dimethyltin(IV) compounds the opposite effects of the coordination number of tin, which tends to increase $^{1,2}J$ and the low C−Sn−C angle, which contributes to decrease $^{1,2}J$, are responsible for the deviation from the eqs 1–3. Finally, the calculated coupling constants for model **11d** (Table 4) are also in rather good agreement with the experimental values.

Table 4. Calculated C−Sn−C Angle θ (Degrees), Sn−C, Sn−N, and Sn−O Average Distances, *d*, (pm), ^1Js and ^2Js Coupling Constants (Hz) and Relative mPW1PW91 Energy, ΔE (kcal/mol), for the Isomer Models of **11**

	11a	**11b**	**11c**[a]	**11d**[b]
d(Sn−C)	217	216	218	215.9
d(Sn−N)	259	227	242	235.0
d(Sn−O)	210	213.6	214	211.1
θ_{calc}[c]	138.9	127.5	109.9	110.7
θ_{est}[d]	146.1; 140.0	133.2; 122.9	129.3; 117.7	131.1; 116.6
^1J[e]	−790.3	−643.6	−599.5	−619.9
^2J[e]	86.74	73.03	67.48	66.20
ΔE	+5.5	+12.9	0.0	

[a] Fully optimized geometry (B3LYP) corresponding to the crystallographic structure. [b] X-ray[58] structure with optimized hydrogen positions (B3LYP). [c] θ_{cal} = C−Sn−C angle of the optimized, or X-ray, structures. [d] θ_{est} = C−Sn−C angle estimated from eqs 1 and 2 from the calculated ^1J and ^2J, respectively. [e] Calculated $^{1,2}J$s were obtained using the mPW1PW91 functional. Experimental values are 632 and 71.2 Hz, respectively.[17,64]

For $Me_2Sn(Trop)_2$, three models have been considered, for the cis, trans, and X-ray structures, respectively. In Scheme 3, we show the structures of the cis and trans isomers respectively. Coordinates are reported in the Supporting Information.

A very similar behavior to the $Me_2Sn(Ox)_2$ complex is found for $Me_2Sn(Trop)_2$, and the results are reported in Table 5. We note that the calculated $^{1,2}J$s obtained for the putative trans isomer, although in disagreement with the experimental values, satisfy eqs 1–3; in contrast, the results obtained for the cis isomer, in rather good agreement with the experiments, do not match the trend expected from the above relationships.

(58) Kepert, D. L *Inorg. Chem.* **1973**, *12*, 1944–1949.
(59) Schlemper, E. O *Inorg. Chem.* **1967**, *6*, 2012–2017.
(60) (a) Braham, S. K.; Nelson, W. H. *Inorg. Chem.* **1982**, *21*, 4076–4079. (b) Howard, W. F., Jr.; Crecely, R. W.; Nelson, H. N. *Inorg. Chem.* **1985**, *14*, 2204–2208.
(61) (a) Camacho-Camacho, C.; Contreras, R.; Nöth, H.; Bechmann, M.; Sebald, A.; Milius, W.; Wrackmeyer, W. *Magn. Reson. Chem.* **2002**, *40*, 31–40. (b) Deák, A.; Király, P.; Tárkányi, G. *Dalton Trans.* **2007**, 234–239.
(62) Lockhart, T. P.; Davidson, F. *Organometallics* **1987**, *6*, 2471–2487.
(63) Ma, C.; Han, Y.; Li, D. *Polyhedron* **2004**, 1207–1216.
(64) Otera, J.; Hinoishi, T.; Kawabe, Y.; Okawara, R. *Chem. Lett.* **1981**, 273–274.

Scheme 3. *cis*- and *trans*-Dimethyltin(IV) Isomers of $Me_2Sn(Trop)_2$

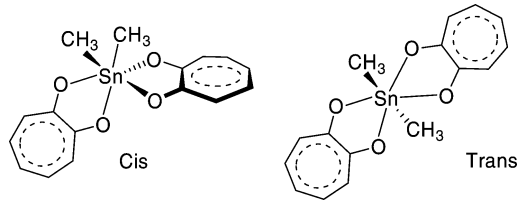

Table 5. Calculated C−Sn−C Angle θ (Degrees), Sn−C, and Sn−O Average Distances, *d*, (pm), ^1Js and ^2Js Coupling Constants (Hz) and Relative mPW1PW91 Energy, ΔE (kcal/mol), for the Isomer Models of $Me_2Sn(Trop)_2$

	trans	cis	X-ray[a]
Sn−C	216.1	217.8	213.5
Sn−O	225.4	221.6	217.3
θ_{calcd}[b]	144.9	109.0	109.3
θ_{est}[c]	150.8; 148.9	131.7; 118.1	124.6; 126.4
^1J[d]	−843.7	−626.0	−545.1
^2J[d]	92.4	68.0	76.3
ΔE	+2.7	0.0	

[a] Geometrical parameters from ref.[61] [b] θ_{calcd} = C−Sn−C angle of the optimized, or X-ray, structures. [c] θ_{est} = C−Sn−C angle estimated from eqs 1 and 2 from the calculated ^1J and ^2J, respectively. [d] Calculated $^{1,2}Js$ with the mPW1PW91 functional. Experimental values are 643 and 72.2 Hz, respectively.[17,64b] Two different ^1J values are reported for the solid state of $Me_2Sn(Trop)_2$ in ref.[64a] of 600 and 629 Hz, respectively, for the two molecules in the unit cell. These values are in better agreement with the results of the calculations.

Scheme 4. *cis*- and *trans*-Dimethyltin(IV) Isomers of $Me_2Sn(Phen)(mnt)$

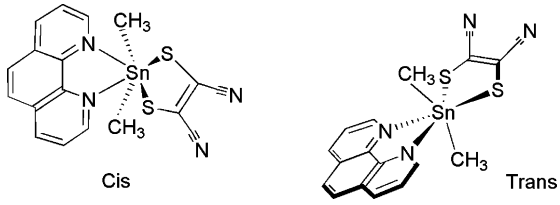

Finally, also for $Me_2Sn(Phen)(mnt)$ we have calculated the coupling constants for the cis and trans optimized structures, Scheme 4, as well as for the X-ray structure. Results are reported in Table 6.

The calculated ^2J for the correct cis configuration is within a few hertz of the experimental value, which is consistent with the accuracy of the computational protocol. In contrast, the calculated value for the hypothetical trans conformer is off by more than 18 Hz.

It is noteworthy that ^2Js, analogously to what is reported in ref,[17] seems to better track θ with respect to the corresponding ^1Js for this class of compounds.

Finally, in the Supporting Information we report the results for the cis isomer (concerning the ligands orientation) of **14** (**14b**); the calculated results are very similar to those obtained for the trans isomer because the methyl groups are arranged similarly in both cases.

For **2**, **3**, **4, 5**, **9**, **12**, **16**, and **17**, further calculations were carried out using the 6-311G** basis set for selenium, sulfur, chlorine, phosphorus, and bromine; the calculated values were, in most cases, almost identical to those obtained with the 6-31G** basis set, the difference being no more of 2% (Supporting Information)

Table 6. Calculated C−Sn−C Angle θ (Degrees), Sn−C, and Sn−N Average Distances, *d*, (pm), ^1Js and ^2Js Coupling Constants (Hz) and Relative mPW1PW91 Energy, ΔE (kcal/mol), for the Isomer Models of $Me_2Sn(Phen)(mnt)$

	trans	cis	X-ray[a]
Sn−S	254.1	256.9	259.3
Sn−N	285.6	253.7	238.8
θ_{calcd}[b]	141.2	104.1	109.7
θ_{est}[c]	130.25; 135.3	120.4; 111.8	115.4; 120.3
^1J[d]	−690.9	−497.5	−441.9
^2J[d]	83.4	59.4	70.4
ΔE	+4.4	0.0	

[a] Geometrical parameters from ref.[63] [b] θ_{calcd} = C−Sn−C angle of the optimized, or X-ray, structures. [c] θ_{est} = C−Sn−C angle estimated from eqs 1 and 2 from the calculated ^1J and ^2J, respectively. [d] Calculated $^{1,2}Js$ with the mPW1PW91 functional. Experimental value of ^2J is 65 Hz.[63]

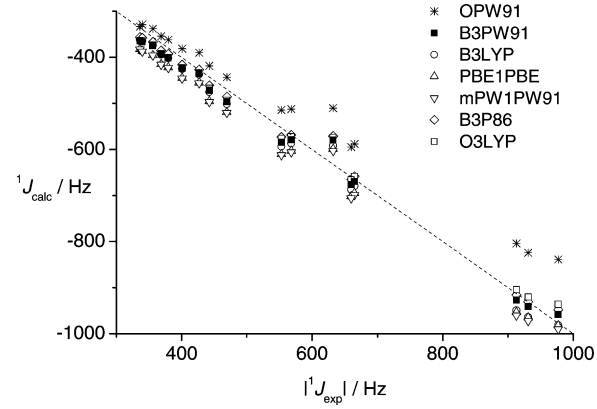

Figure 3. Correlation between calculated and experimental $^1J(^{119}Sn,^{13}C)$ of model systems of Scheme 1, PBE1PBE optimized geometries (Table S5 in the Supporting Information). (Dashed line) ideal correlation $y = -x$.

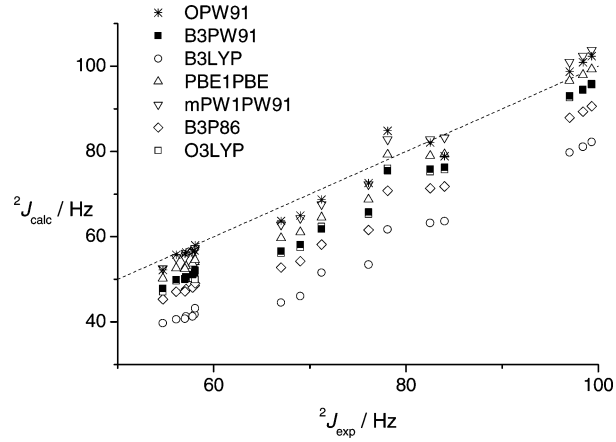

Figure 4. Correlation between calculated and experimental $^2J(^{119}Sn,^1H)$ of model systems of Scheme 1, PBE1PBE optimized geometries (Table S6 in the Supporting Information). (Dashed line) ideal correlation $y = x$.

Model Systems with PBE1PBE Geometries. In Tables S5 and S6 in the Supporting Information, we report the calculated $^1J(^{119}Sn,^{13}C)$ and $^2J(^{119}Sn,^1H)$ for the same set of molecules and selected functionals used above, but now using geometries optimized with the PBE1PBE functional.

Comparing Figures 3 and 4 with Figures 1 and 2, respectively, we note that the effect of the geometry is, indeed, significant; however the overall correlation of $^{1,2}Js$ obtained from the B3LYP geometries does not differ substantially from the one obtained from the PBE1PBE geometries (statistical data in Table 7). The performance of

Table 7. Statistical Correlation Parameters of $^1J(^{119}Sn,^{13}C)$ and $^2J(^{119}Sn,^1H)$ Data, PBE1PBE Geometries: Linear Fit $J_{calcd} = a + bJ_{exptl}$, Correlation Coefficient, R^2, Mean Absolute Error, MAE, Defined as $\Sigma_n|J_{calcd} - J_{exptl}|/n$ and Maximum Absolute Error, E_{max}

	$^1J(^{119}Sn,^{13}C)$					$^2J(^{119}Sn,^1H)$				
function	*a* (Hz)	*b*	R^2	MAE (Hz)	E_{max} (Hz)	*a* (Hz)	*b*	R^2	MAE (Hz)	E_{max} (Hz)
OPW91	−52.3	−0.8118	0.9918	52.0	138.5	−5.99	1.0735	0.9754	2.35	6.74
B3PW91	−39.1	−0.9529	0.9921	21.4	52.7	−11.09	1.0604	0.9821	6.75	10.86
B3LYP	−24.7	−0.9925	0.9928	25.3	40.3	−14.50	0.9517	0.9707	17.97	22.94
PB1PBE	−57.3	−0.9605	0.9912	39.3	57.1	−9.84	1.0837	0.9821	3.96	7.94
mPW1PW91	−53.9	−0.9720	0.9914	41.8	59.2	−9.91	1.1300	0.9840	2.61	4.72
B3P86	−31.7	−0.9488	0.9925	14.8	29.2	−10.85	1.0037	0.9796	10.58	14.73
O3LYP	−51.4	−0.9178	0.9926	20.4	57.9	−12.54	1.0743	0.9816	7.20	11.53

the various functionals is rather similar, particularly for ^2Js, whereas for ^1Js the results obtained from the PBE1PBE geometries are systematically slightly higher in magnitude than the corresponding values obtained from the B3LYP geometries.

The general observation, therefore, is that even a relatively low level of theory as that one used here is capable of predicting spin−spin coupling constants involving tin with a high degree of accuracy. Furthermore, we note that the protocols treat equally well those cases where the Lockhart−Manders relations fail (cis methyl configuration) and dimethyltin halides, which were found to follow a slightly different curve from eq 2.[17]

Application of the Protocols to Aquodimethyltin(IV) Ion and Other Complexes of Biological Interest. Interaction between organotin(IV) moieties and molecules of biological interest has been reviewed[2] and among them, interactions with aminoacids[7] or peptides,[8] and carbohydrates and related derivatives[29,30,65] were investigated because of their relevant biological importance. We have studied (i) the aquodimethyltin(IV) ion, $Me_2Sn(H_2O)_n^{2+}$, as a test case due its greater Lewis acidity; (ii) the complex of Me_2Sn^{2+} with D-ribonic acid in water; and (iii) the complexes, in water, of Me_2Sn^{2+} with the dipeptides glycylglycine and glycylhistidine. These systems also allow us to investigate in detail the effect of water, which has a strong coordinating power toward the acidic Me_2Sn^{2+} moiety, using explicit solvent molecules and the polarizable continuum model (PCM).[40] We have considered two different protocols: the first, protocol 1, is based on B3LYP geometries and NMR properties calculated with the mPW1PW91 functional; this gives good values of ^2Js, within a few hertz of the experimental data, Table 3, and satisfactory results for the ^1Js; for the second, protocol 2, we use PBE1PBE geometries and we calculate NMR properties with the B3PW91 functional, which seems to be a good compromise for the calculation of both ^1Js and ^2Js.

Table 8. Calculated $^2J(^{119}Sn,^1H)$ Coupling Constants (Hz), for the Aquodimethyltin(IV) Ion Using Various Models and the Two Protocols

		$^2J(^{119}Sn,^1H)^b$	
	model[a]	protocol 1	protocol 2
A	$Me_2Sn(H_2O)_4^{2+}$	74.3	66.4
A′	$Me_2Sn(H_2O)_4^{2+}$	90.2	81.5
B	$Me_2Sn(H_2O)_8^{2+}$	93.0	83.7
B′	$Me_2Sn(H_2O)_8^{2+}$	101.4	91.5
C	$Me_2Sn(H_2O)_{10}^{2+}$	95.2	86.2
C′	$Me_2Sn(H_2O)_{10}^{2+}$	101.8	
D	$Me_2Sn(H_2O)_4^{2+}$	84.3	
D′	$Me_2Sn(H_2O)_4^{2+}$	100.6	88.8

[a] NMR properties were calculated with and without PCM. In the latter case the model is denoted by a prime. [b] Experimental value $^2J(^{119}Sn,^1H)$ = 106 Hz, from ref.[66]

Aquodimethyltin(IV) Ion. The high affinity of tin(IV) for oxygen donors is responsible for a strong interaction between tin and four water molecules in its first coordination sphere, as indicated by Raman, IR, and NMR techniques.[66] Thus, to investigate the effect of the solvent we have selected model systems composed of Me_2Sn^{2+} coordinated to four water molecules, and larger clusters of 8 and 10 water molecules, whose gas-phase optimized structures are shown in Figure 5. For all systems, the calculation of the NMR properties has been run in the gas phase and with PCM (models A, B, C, and A′, B′, C′, respectively). We have also optimized the structure of the smallest cluster using PCM to test the importance of long-range solvent effects during the optimization (model D) and in the following ^2J calculation (model D′). The results are reported in Table 8.

The average calculated Sn−O distance of $Me_2Sn(H_2O)_4^{2+}$ optimized in the gas phase (model A) is 234 pm, and the geometry is almost octahedral with a C−Sn−C angle of 177° (the θ value estimated by means of the Lockhart equation and the experimental ^2J is 174°). However, by considering

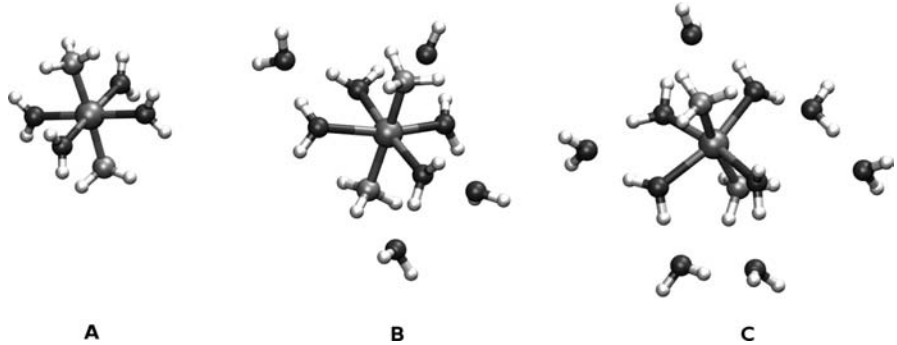

Figure 5. Gas-phase optimized structures (B3LYP) of: (A) $Me_2Sn^{2+}\cdot 4H_2O$; (B) $Me_2Sn^{2+}\cdot 8H_2O$; (C) $Me_2Sn^{2+}\cdot 10H_2O$ model clusters.

Scheme 5. Fischer Projection of D-Ribonic Acid

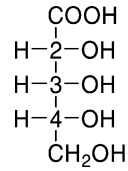

only the first solvation shell the calculated ^2J coupling constant is not in agreement with the experimental value, being underestimated by more than 30 Hz (model A).

Better results are obtained after inclusion of long-range solvent effects (models B′, C′, D′ with protocol 1): the solvent effect on the geometry can be modeled either by increasing the number of explicit water molecules or by running the optimization with the PCM scheme. In both cases, the average Sn−O distance with the first four water molecules is reduced to 228 and 230 pm for models C and D, respectively. The subsequent ^2J calculation, then, also needs to be run including the PCM solvent reaction field. Results obtained with protocol 2 are somewhat worse. This is, however, expected on the basis of the correlations of the various protocols obtained for the model systems discussed in the previous section.

Me_2Sn^{2+} Complex with D-Ribonic Acid. D-Ribonic acid, Scheme 5, in water coordinates to dimethyltin(IV) via two oxygen atoms, namely a carboxylic oxygen and the deprotonated hydroxy oxygen, O3.

The structure of the complex in solution was determined from ^{1}H, ^{13}C, and ^{119}Sn NMR data as well as from DFT calculations.[29] Moreover, the ^{1}H NOEs, the presence of two ^{119}Sn resonances, and ^{13}C line-width analysis also clearly indicated the existence of a dimeric species, although the monomer and dimer were in a fast exchange regime on the NMR time scale. For the dimeric species, NMR data suggested that the OH4 group of one moiety was interacting with the tin atom of the other moiety.

Thus, two different monomer models have been considered with one (**M1**) and two (**M2**) explicit water molecules interacting with tin. For the dimeric species, similar to what was reported in our previous work,[29] we have considered a case (model **D1**) where the two tin centers are non-equivalent because one tin atom, namely Sn(**b**), is interacting with one water molecule (Figure 6). In a second model (**D2**), both tin centers are interacting with the OH4 group, and, again, Sn(**b**) is also coordinated by an additional water molecule.

Structural data reported in Table 9 show that the optimizations performed with protocol 1 generally lead to longer Sn−O distances, and, therefore, smaller C−Sn−C angle values, with respect to protocol 2. Nevertheless, as expected on the basis of the results reported in Tables 3 and 4, protocol 2 gives calculated ^2Js lower than those obtained with protocol 1.

Monomer models with one (**M1**) or two (**M2**) explicit water molecules show a noticeable difference in the calculated ^2Js and a significant improvement, by about 12 Hz, is obtained by considering two explicit water molecules. We note that, in contrast to the highly charged aquodimethyltin(IV) ion, this is a neutral complex; therefore the Lewis acidity of tin is expected to be strongly reduced and the long-range solvent effect to be somewhat lower than in the case of the aquodimethyltin(IV) ion. In fact, the inclusion of the solvent reaction field through the PCM model (**M2′**) has a relatively small effect on the calculated coupling constant.

As far as the dimer form of $Me_2SnRibn$ is concerned, the calculation shows that both the water molecule and the OH4 group (Sn(**b**) in **D1** model and Sn(**a**) in **D2** model, respectively) affect in a similar way the ^2J coupling constant, giving, in both cases, calculated values in agreement with the experimental data, and then a competitive exchange with tin is conceivable. The other cases regarding the dimeric $Me_2SnRibn$, where neither or both the OH4 and H_2O interact with tin (Sn(**a**) in **D1** and Sn(**b**) in **D2**, respectively) give calculated ^2J in disagreement with the experimental value.

To summarize, we note that the best agreement with the experimental value is obtained for those models where the tin centers are hexa-coordinated by water molecules and/or a suitable OH group. This result may be expected on the basis of the strong coordinating power of water toward tin(IV).

As for the aquodimethyltin(IV) ion, protocol 2 does not perform very well for the calculation of ^2J. All calculated values are somewhat underestimated compared to the experimental ones.

Me_2Sn^{2+} Complexes with Dipeptides. The systems we have investigated are two complexes studied by Surdy et al.[7a] The authors reported that at pH around 7 and 6, respectively, the most abundant species in water solution is a 1:1 complex of dimethyltin(IV) with glycylglycine ($Me_2SnGlyGly$) and glycylhistidine ($Me_2SnGlyHis$). The complexes are electrically neutral, and the structures have been proposed according to a $\{COO^-, N^-, NH_2\}$ coordination mode of the ligand after deprotonation of the carboxylic oxygen and the amide nitrogen.

For the smaller $Me_2SnGlyGly$ system, we have considered the structure reported in ref[7a] and shown in Figure 7 and larger systems obtained with explicit inclusion of water molecules. Some relevant geometrical parameters, together with the calculated one- and two-bond spin−spin coupling constants, are reported in Table 10. First, we note that the results obtained for the bare complex do not agree with experimental data. Both protocols underestimate (in magnitude) the $^{1,2}J$ experimental values. Thus, we have considered the inclusion of an explicit water molecule in the coordination sphere of tin. The agreement is significantly improved; in particular with protocol 1 we obtain results very close to the experimental data. Inclusion of an additional water molecules slightly further improves the result for ^2J while worsening the agreement for ^1J. We recall, however, that protocol 1 might underestimate ^2Js by a few hertz, at least in this range of values (Table 3). These results indicate that,

(65) (a) Bertazzi, N.; Bruschetta, G.; Casella, G.; Pellerito, L.; Rotondo, E.; Scopelliti, M. *Appl. Organomet. Chem.* **2003**, *17*, 932–939. (b) Szorcsik, A.; Nagy, L.; Gyurcsik, B.; Vankó, G.; Krämer, R.; Vertes, A.; Yamaguchi, T.; Yoshida, K. *J. Radioanal. Nucl. Chem.* **2004**, *260*, 459–469.

(66) McGracy, M. M.; Tobias, R. S. *Inorg. Chem.* **1964**, *3*, 1157–1163.

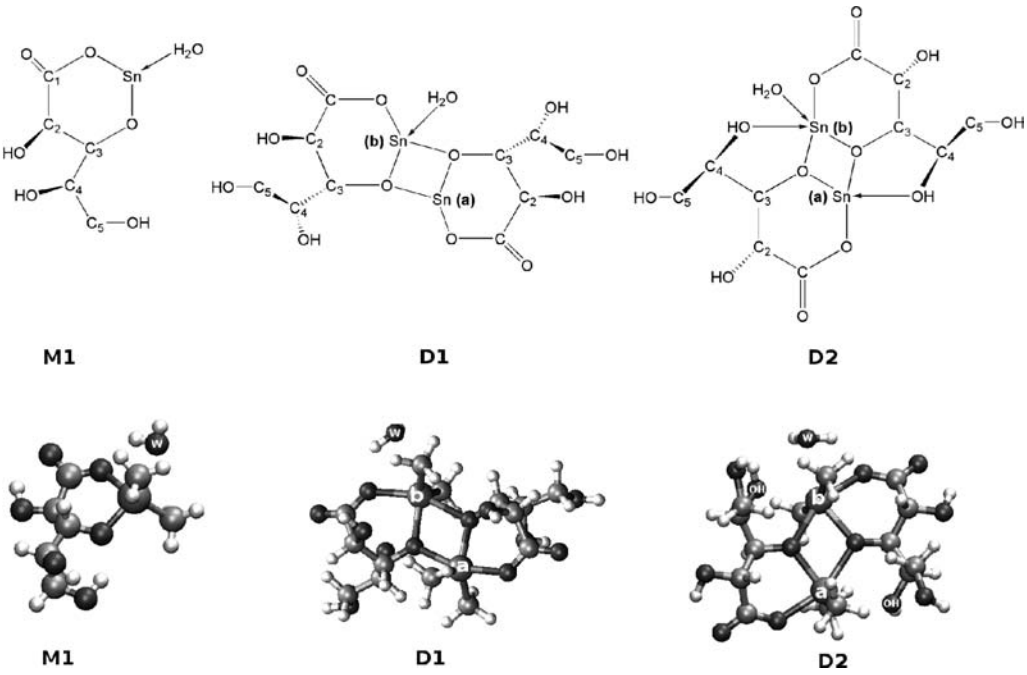

Figure 6. Gas-phase optimized structures (B3LYP) of the monomeric and dimeric forms of $Me_2SnRibn$. The OH groups and water molecules interacting with tin are all labeled. **M1**, $Me_2SnRibn$ with one water molecule coordinated to tin; **D1**, dimer of $Me_2SnRibn$ with one water molecule coordinated to Sn(**b**); **D2**, dimer of $Me_2SnRibn$ with both tin centers interacting with the OH4 group and one water molecule coordinated to Sn(**b**).

Table 9. Calculated C−Sn−C Angles θ (Degrees), Selected Sn−O Distances d (pm), and Calculated and Experimental Coupling Constants $^2J(^{119}Sn,^1H)$ (Hz) for the Studied Models

		protocol 1			protocol 2		
model[a]	compound	θ[b]	d[c]	^2J	θ[b]	d[c]	^2J
M1	$Me_2SnRibn+H_2O$	126.6	252.1	70.6			
M2	$Me_2SnRibn+2H_2O$	136.3	258.7; 262.7	82.8	137.5	253.8; 256.3	76.0
M2′	$Me_2SnRibn+2H_2O$+PCM[d]	136.3	258.7; 262.7	84.1			
D1	Me_2Sn(**a**)Ribn	123.7		75.1	123.3		68.2
	Me_2Sn(**b**)$Ribn+H_2O$	134.1	287.5	86.6	135.8	273.3	80.2
D2	Me_2Sn(**a**)Ribn+OH[e]	141.8	270.3	87.8	142.3	264.2	80.0
	Me_2Sn(**b**)Ribn+OH, H_2O[e]	164.1	250.8; 257.1	105.7	165.2	246.6; 250.6	96.5

[a] **M** = monomer, **D** = dimer; experimental data from ref,[29] $^2J = 87 \pm 3$ Hz. [b] Calculated C−Sn−C angle. [c] The values are referred to calculated Sn−O distances for the OH group and/or for one or two H_2O molecules, respectively. [d] PCM was used for the calculation of the NMR properties. [e] OH = intramolecular interaction between the tin center and the OH4 group of the dimeric form of $Me_2SnRibn$.

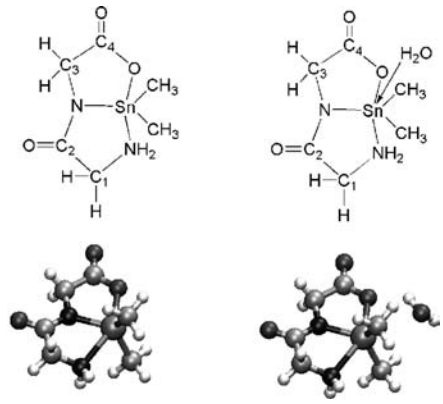

Figure 7. (Top) Structure with numbering of the carbons atoms and (bottom) gas-phase optimized geometry (B3LYP) of the $Me_2SnGlyGly$ and $Me_2SnGlyGly \cdot H_2O$ complexes.

in water solution, tin is coordinated by just one water molecule reaching hexa-coordination (Figure 7).

It is also noteworthy that the solvent effect cannot be properly accounted for by PCM alone. For the bare complex the use of PCM in the coupling calculation does not represent a substantial improvement; the same conclusion holds for the case of two water molecules (see Table 10).

In ref. [7a] some long-range spin−spin couplings of tin with protons and carbons, namely a $^3J(^{119}Sn,^1H3)$ and ^2J couplings with C2, C3, and C4, respectively, were also reported. The calculated values are shown in Table 11 for the same structures and methods of Table 10.

Considering the model with one explicit water molecule, we note a good agreement concerning $^3J(^{119}Sn,^1H)$ while $^2J(^{119}Sn,^{13}C)$ appear underestimated. Caution is therefore recommended in extending the above protocols to long-range coupling constants between tin and carbon, particularly in cases where multiple paths are available for coupling.

Finally, for the $Me_2SnGlyHis$ complex two methyl ^{13}C signals for the dimethyltin(IV) moiety have been reported,[7a] one of them being particularly shielded ($\delta = -0.22$). We have then optimized two conformers: the most stable, by about 4 and 5 kcal/mol at the level theory of protocols 1 and 2 respectively is conformer A, where a methyl group,

Table 10. Calculated C−Sn−C Angles θ (Degrees), Sn−N and Sn−O Distances d (pm), and $^1J(^{119}Sn,^{13}C)$ and $^2J(^{119}Sn,^1H)$ Coupling Constants (Hz) for $Me_2SnGlyGly$

	protocol 1					protocol 2				
N H_2O	θ	d(Sn−N)[a]	d(Sn−O)[b]	^1J	^2J	θ	d(Sn−N)[a]	d(Sn−O)[b]	^1J	^2J
0	120.6	2.465		−589.2	68.7	120.8	243		−572.0	62.7
0+PCM	120.6	2.465		−608.1	70.1					
1	127.9	2.498	2.870	−678.7	77.1	129.4	247	271	−687.4	70.9
2	135.5	2.539	2.588	−769.1	82.1	136.0	250	252	−759.3	75.0
2+PCM				−791.5	84.0					
3	137.9	2.565	2.490	−794.5	84.6	138.9	251	244	−785.2	77.9
exptl[c]				656.9	82.2				656.9	82.2

[a] Amide nitrogen. [b] Closest water molecule. [c] From ref,[7a] absolute values for ^1J.

Table 11. Calculated $^2J(^{119}Sn,^{13}C)$ and $^3J(^{119}Sn,^1H)$ Coupling Constants (Hz) for the $Me_2SnGlyGly$, Protocol 1

N H_2O	^3J(Sn−H3)[a]	^2J(Sn−C1)	^2J(Sn−C2)	^2J(Sn−C3)	^2J(Sn−C4)
0	−26.6	3.1	−24.6	−17.1	3.0
1	−21.1	2.2	−16.1	−12.1	−0.2
2	−17.1	1.8	−10.0	−8.4	0.4
2+PCM	−14.2	1.3	−10.0	−9.0	1.6
3	−15.7	1.7	−7.4	−7.5	0.4
exptl[b]	22.5		34.9	20.7	∼11

[a] Average value. [b] From ref.[7a]

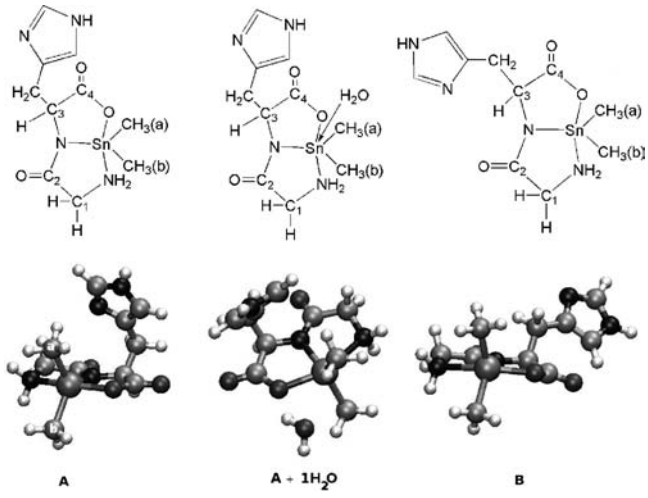

Figure 8. (Top) Structures and (bottom) gas-phase optimized geometries (B3LYP) of the A and B conformers of the $Me_2SnGlyHis$ complex and of the monohydrated form of A.

labeled **a** in Figure 8, is facing the aromatic ring of histidine. This arrangement also accounts for the strong shielding of the methyl group itself.

The calculated $^{1,2}J$s for the complex with no additional water molecules are in poor agreement with experiments, using both protocols. Moreover, for isomer B the relative magnitude of the two nonequivalent ^1Js is incorrect. Therefore, we have only considered the most stable isomer A with explicit water molecules. As for the case of the $Me_2SnGlyGly$ complex, a satisfactory agreement is obtained by considering just one explicit water molecule (Tables 12 and 13). It is also comforting that the relative magnitude of the calculated ^1Js with the two non-equivalent methyl groups is now correctly reproduced. As expected on the basis of the general performance of protocols 1 and 2, a rather good agreement is obtained for ^2Js with protocol 1, whereas protocol 2 performs slightly better for ^1Js.

Conclusions

The results reported in this work show the effectiveness of some nonrelativistic DFT protocols for the calculation of $^1J(^{119}Sn,^{13}C)$ and $^2J(^{119}Sn,^1H)$ coupling constants in di- and trimethyltin(IV) compounds for tetra-, penta- and hexa-coordinated tin. For both B3LYP and PBE1PBE optimized geometries, quite a good performance in the $^{1,2}J$s calculation was found even if it was not possible to propose a unique functional. As a consequence of these findings, two protocols have been tested to validate the NMR solution structural studies of some dimethyltin(IV) complexes. Our results show that even in the presence of a coordinating solvent like water as well as in the presence of intra/intermolecular interactions involving tin, the proposed protocols can be usefully employed for the prediction of spin−spin coupling constants, or, in a reverse fashion, for the validation of structures based on the comparison of experimental and calculated values. This is of special interest because the DFT results are valid also in those cases where the Lockhart−Manders relations fail, namely in the presence of cis configuration of the two methyl groups, for hexa-coordinated dimethyltin(IV) moieties; moreover, whereas the Lockhart−Manders relations need to be parametrized differently for the case of di- and trimethyltin halides,[17] DFT methods are equally valid for any set of ligands and donor atoms, comprising oxygen, nitrogen, sulfur, selenium, chlorine, and bromine. As expected, coupling constants of formally tetra- or penta-coordinated complexes are strongly influenced by the coordination of water molecules that need to be explicitly included in the calculation.

It is rather surprising that a relatively low level of theory such as that used here, particularly concerning the basis set, provides such a good correlation with calculated values. Several approximations have been made: (i) relativistic effects have been neglected, although they have been found to be significant for spin−spin coupling constants involving tin in organo-tin(IV) compounds; (ii) the effect of tight *s* functions and larger basis sets should be investigated in more detail. However, the size of the systems that we have considered does not allow us to extend the basis set significantly keeping, at the same time, the protocols useful from a practical point of view; (iii) DFT is an approximate method because electron correlation is not fully accounted for. However, the use of true correlated ab initio methods for such cases is prohibitive.

Table 12. Calculated C−Sn−C Angles θ (Degrees), Sn−N and Sn−O Distances d (pm), and $^1J(^{119}Sn,^{13}C)$, $^2J(^{119}Sn,^1H)$ Coupling Constants (Hz) for the Me_2Sn(IV) Complex with GlyHis, Protocol 1

N H_2O	θ	d(Sn−N)[a]	d(Sn−O)[b]	^1J(Sn−Ca)	^1J(Sn−Cb)	^2J(Sn−Ha)	^2J(Sn−Hb)
A	119.4	209.9		−595.0	−584.1	72.3	66.8
B	120.1	210.3		−573.9	−605.4	68.2	65.5
A+1H_2O	123.0	211.1	321.2	−635.1	−615.1	80.8	71.4
A+2H_2O	134.7	213.3	264.3	−785.8	−733.4	90.2	76.3
exptl[c]				663.4	646.6	80.2	80.7

[a] Amide nitrogen. [b] Closest water molecule. [c] From ref.,[7a] absolute values for ^1J.

Table 13. Calculated C−Sn−C Angles θ (Degrees), Sn−N and Sn−O Distances d (pm), and $^1J(^{119}Sn,^{13}C)$, $^2J(^{119}Sn,^1H)$ Coupling Constants (Hz) for the Me_2Sn(IV) Complex with GlyHis, Protocol 2

N H_2O	θ	d(Sn−N)[a]	d(Sn−O)[b]	^1J(Sn−Ca)	^1J(Sn−Cb)	^2J(Sn−Ha)	^2J(Sn−Hb)
A	119.3	208.2		−551.4	−541.3	63.1	58.2
B	120.3	208.6		−529.7	−563.7	59.5	59.6
A+1H_2O	126.8	209.9	287.2	−644.0	−612.7	73.6	63.1
A+2H_2O	135.6	211.6	257.0	−736.7	−696.2	79.0	67.1
exptl[c]				663.4	646.6	80.2	80.7

[a] Amide nitrogen. [b] Closest water molecule. [c] From ref[7a] absolute values for ^1J.

In summary, although the predictive power of the protocols we have presented is very likely to be the result of errors compensation, such protocols, particularly protocol 1, can indeed be exploited to select or discard putative structures of di- or trimethyltin(IV) complexes on the basis of the comparison of calculated and experimental $^1J(^{119}Sn,^{13}C)$ and $^2J(^{119}Sn,^1H)$ coupling constants.

Acknowledgment. We thank Prof. A. Bagno, Università di Padova, for many useful comments. Calculations were run on the Linux cluster of the Laboratorio Interdipartimentale di Chimica Computazionale, Università di Padova, and on several Linux PC.

Supporting Information Available: Table of ^1Js and ^2Js for model systems, Cartesian coordinates of all compounds with SD, PSO, DSO, and FC contributions to $^{1,2}J$s. This material is available free of charge via the Internet at http://pubs.acs.org.

IC8000976